

## Supporting Information

# A general strategy for the obtainment of biodegradable polymer shelled microbubbles as theranostic device

Sabrina Capece, Ester Chiessi, Roberta Cavalli, Pierangela Giustetto,  
Dmitry Grishenkov and Gaio Paradossi \*

*Received (in XXX, XXX) Xth XXXXXXXXXX 20XX, Accepted Xth XXXXXXXXXX 20XX*  
DOI: 10.1039/b000000x

Contents	Page number
1. General information .....	3
2. Synthesis of dextran methacrylate derivative .....	3
3. Synthesis of hyaluronic acid methacrylate derivative .....	4
4. Synthesis of perfluorocarbon filled vesicles .....	4
5. Preparation of RBITC-labelled vesicles .....	4
6. Acoustic droplet vaporization (ADV) by application of ultrasounds .....	5
7. Ultrasounds mediated fracture of MBs .....	5
8. Thermal and US sensitivity of dex/p(MA-co-NiPAAm) vesicles .....	5
9. Micro-Ultrasound characterization .....	5
10. Biodegradability of DexMA50 vesicles: lysozyme and dextranase effect .....	8
11. <sup>1</sup> H NMR spectrum of methacrylated-dextran .....	9
12. <sup>1</sup> H NMR spectrum of methacrylated-hyaluronic acid .....	10
13. Table S1: Composition (a) and parameters (b) set in vesicles synthesis .....	11
14. Table S2: SP100 parameters set in ultrasound treatment of vesicles.....	12

15. Picture of ultrasound mediated fracture of DexMa50 vesicles .....	12
16. Picture of ultrasound triggered ADV of Dex/p(MA-co-NiPAAm) vesicles .....	13
17. Experimental set-up designed to simulate a harmonic imaging technique.....	13
18. Pictures related to harmonic imaging technique simulation .....	14
19. Table S3: Vevo <sup>®</sup> 2100 parameters set in micro-ultrasound experiment.....	15
20. Picture of micro-ultrasound characterization performed by Vevo <sup>®</sup> 2100 .....	15
References .....	16

## 1. General information

N-isopropylacrylamide (NiPAAm) was recrystallized from n-hexane prior to use. Irgacure 2959<sup>®</sup> was a BASF (Kaisten, CH) product and Epikuron 200<sup>®</sup> was purchased from Cargill (Hamburg, GE). Hyaluronic acid ( $M_w$  700000 g/mol) was a kind gift from Fidia Farmaceutici S.p.A. (Abano Terme, Italy). Solvents were from Carlo Erba Reagents (Milan, Italy). All other chemicals were Sigma Aldrich (Steinheim, GE) products. Milli-Q water (18.2 M $\Omega$ ·cm) was produced by a deionization apparatus PureLab from USF (Perugia, Italy). All <sup>1</sup>H NMR spectra were carried out at a polymer concentration of 7 mg/mL in D<sub>2</sub>O using a Bruker Avance 300 MHz spectrometer. Confocal Laser Scanning Microscope (CLSM) images were collected using a Nikon Inverted Microscope Eclipse model Ti-E from Nikon Instrument (Japan), equipped with: 60x/1.4 oil immersion objective, Argon-Ion laser (488 nm) (Melles Griot, Carlsbad, CA, USA), Helium-Neon laser (543.5/633 nm) (Spectra Physics, Mountain View, CA, USA). Ultrasounds studies were carried out by Sonidel SP100 Sonoprotator from SONIDEL<sup>™</sup> (Dublin, IE). Vevo<sup>®</sup> 2100 system of VisualSonics Instrument (Amsterdam, NL). Micro-Ultrasound characterization was performed using two focused ultrasound transducers: 2.2 MHz transducer (diameter 13 mm, focal length 50mm and -6 dB bandwidth 1.8 - 3.4 MHz) from Krautkramer, Gamma Series, Krautkramer Inc., (Lewistown, PA, USA) and 5 MHz transducer V309 (diameter 13 mm, focal length 50 mm and -6 dB bandwidth 3.43 - 6.77 MHz) from Panametrics (Waltham, MA, USA). Two attenuators, RA-31 (7 dB) and RA-32 (40 dB) from Ritec Inc. (Warwick, RI, USA) were used to vary the intensity of the electrical signal exciting the transducer. Studies of Nonlinear Acoustic Phenomena (SNAP) were realized by the computer-controlled system SNAP Mark IV from Ritec Inc., (Warwick, RI, USA). ImageJ software package (<http://rsb.info.nih.gov/ij/>) was used to count vesicles and custom developed software (Matlab, The Mathworks inc., Natick, MA, USA) was used for the ultrasound signal intensity analysis.

## 2. Synthesis of dextran methacrylate derivative

Typically, 5 g of dextran ( $M_w$  35000-40000 g/mol),  $3.1 \cdot 10^{-2}$  moles of repeating units, was dispersed in 100 mL of dimethylsulfoxide (DMSO) under nitrogen atmosphere. 7.59 g of 4-(Dimethylamino)-pyridin (DMAP) ( $6.2 \cdot 10^{-2}$  moles) was added and the mixture was left for 2 hours in the dark under continuous stirring, followed by the addition of 2.2 g of glycidyl methacrylate ( $1.6 \cdot 10^{-2}$  moles). Reaction was carried out for 48 hours at room temperature in the dark under vigorous stirring, and was stopped by neutralizing DMAP with an equimolar amount

of HCl. The product was then purified by extensive dialysis against water and stored as a freeze-dried powder (yield  $\cong$  95%).<sup>1</sup> The acryloyl substitution was assessed by <sup>1</sup>H-NMR spectroscopy, with the presence of acrylate peaks at  $\sim$  5.8 and  $\sim$  6.2 ppm and dextran anomeric proton peak at  $\sim$  5.0 ppm. The degree of substitution (DS), about 50 %, was determined as the ratio of the areas of the acrylate peaks over the proton anomeric peak (Fig. S1). Methacrylated dextran is indicated as DexMA50.

### 3. Synthesis of hyaluronic acid methacrylate derivative

Typically, 1 g of hyaluronic acid ( Mw 700000 g/mol),  $1.9 \cdot 10^{-3}$  moles of repeating units, was first dissolved in a mixture of 200 mL of phosphate buffer solution (0.1 mM pH 7.4) and 67 mL of N,N-dimethylformamide. Then 13.3 g of glycidyl methacrylate ( $9.4 \cdot 10^{-2}$  moles) and 6.7 g of triethylamine ( $6.6 \cdot 10^{-2}$  moles) were added under continuous stirring at room temperature. After 10 days, the mixture was precipitated in a large excess of acetone (20 times the volume of the reaction solution), filtered, dried under vacuum overnight, dialyzed for 3 days against water and then stored as freeze-dried powder (yield  $\cong$  90%).<sup>2</sup> <sup>1</sup>H NMR spectrum of the product was recorded to confirm the obtainment of the methacrylate derivative of hyaluronic acid (HAMA30). The DS was assessed by comparing the areas of the acrylate peaks to the area of the peak assigned to the methyl group ( $\sim$  2 ppm) of N-acetylglucosamine unit of the hyaluronic acid repeating unit (Fig. S2).

### 4. Synthesis of perfluorocarbon filled vesicles

Preparation of perfluorocarbon (PFC) filled vesicles requires a homogenization at high speed obtained by UltraTurrax T-25 (IKA Werke, Staufen, GE). The mixture of the components, described in Tab. S1, was irradiated by a UV lamp at 365 nm with an intensity of 7 mW/cm<sup>2</sup> in an ice bath for 20 min. In all cases Irgacure 2959<sup>®</sup> was used as photoinitiator and added to the other components at a weight ratio of 0.3 with respect to the polymer.

### 5. Preparation of RBITC-labelled vesicles

Rhodamine B isothiocyanate (RBITC) was used as fluorescent probe. RBITC labelling of vesicles required first the washing of vesicles to remove impurities. Washing was carried out by centrifuging the sample for 4 minutes at 1000 rpm, removing the supernatant and adding water. 5  $\mu$ L of a stock solution of RBITC (3 mg/mL) in DMSO was added per mL of washed vesicles

suspension. The mixture was left under slow stirring in the dark for 2 hours. The suspension was then washed twice after centrifugation at 1000 rpm for 1 minute.

### **6. Acoustic droplet vaporization (ADV) by application of ultrasounds**

Effects of ultrasounds (US) application were monitored on RBITC-labelled vesicles. Diameter distribution was analyzed by CLSM on vesicles, immediately after MBs formation and one hour from US application. SP100 sonoprotator was used to test vesicles responsiveness to US at the fixed frequency of 1 MHz. The typical parameters of an ADV ultrasounds experiment, carried out with an effective radiating area of 0.8 cm<sup>2</sup>, are shown in Table S2. In these conditions, the irradiation energy was 7·10<sup>-8</sup> cal/particle. Using the same plasticware and configuration of the experiments, US irradiation increases the temperature of the dispersion of about 0.5 °C. Similar temperature increases, using analogous conditions have been reported in the literature.<sup>3</sup>

### **7. Ultrasounds mediated fracture of MBs**

The possibility to obtain an ultrasounds mediated fracture of DexMa50 MBs was assessed on a RBITC-labelled sample. The set of SP100 parameters used in this type of experiment is shown in Table S2 and Fig. S3 shows the results of the US induced DexMa50 MBs fracture described in the text.

### **8. Thermal and US sensitivity of dex/p(MA-co-NiPAAm) vesicles**

Dex/p(MA-co-NiPAAm) vesicles showed both thermal and US sensitivity. Thermal responsiveness was tested on RBITC-labelled vesicle by injecting a small amount of sample inside a CLSM incubation chamber equipped with a temperature controller. Images were captured at RT and at 45 °C, a temperature above the p(NiPAAm) lower critical solution temperature (LCST). Finally the sample was thermalized back at RT, as reported in the paper. A control experiment was carried out in the same conditions using DexMA50 MBs.

Fig. S4 shows the behavior of dex/p(MA-co-NiPAAm) vesicles before and after US irradiation, with the conditions reported in Table S2.

### **9. Micro-Ultrasound characterization**

Acoustic characterization was performed on a suspension of vesicles diluted to a concentration of 10<sup>7</sup> vesicles/mL, as determined with ImageJ software, in order to avoid multiple scattering. The suspension was injected into an agarose tube with inner diameter of 10 mm. Suspension was regularly exchanged with a fresh one to ensure homogeneous distribution and presence of the

particles inside the insonified volume, as the intersected volume of the two transducers employed in this study is much smaller than the total volume of the agarose tubing, 3 mm<sup>3</sup> and 3 cm<sup>3</sup>, respectively. Acoustic droplet vaporization (ADV) was monitored using two single crystal ultrasound transducers positioned at 90° with respect to each other in the horizontal plane perpendicular to the short axis of the agarose vessel as described in Fig. S5. The focal regions of the emitting and receiving transducers intersected each other: the focused 2.2 MHz transducer was used as an emitter while the focused 5 MHz transducer was used as a receiver. This experimental set-up has been designed to simulate a harmonic imaging technique, where the detection is specific for the second- or ultra-harmonics.

The emitting transducer was driven to oscillation by a computer-controlled system for SNAP. The number of cycles in the excitation square modulated sinusoidal pulse was set to 10 and a pulse repetition frequency (PRF) equal to 100 Hz was chosen to keep duty cycle as low as 0.05%. Two attenuators were used to vary the intensity of the electrical signal exciting the transducer. The peak negative pressure (PNP) was increased stepwise from 0.15 MPa to 2.44 MPa, with a central frequency,  $F_c$ , of 2.2 MHz. According to the definition of mechanical index, MI, (see eq 1) these conditions correspond to a range of MI between 0.1 and 1.63.

$$MI = \frac{PNP (MPa)}{\sqrt{F_c (MHz)}} \quad (1)$$

The receiving signal was first acquired by pulser-receiver (Panametrics PR 5072, Waltham, MA, USA) with the gain set to 40 dB, then digitized by 14 bit waveform digitizer (CompuScope 14200; Gage Applied Technologies, Lockport, IL, USA) at a rate of 80 MHz, and stored in the computer. In total 100 consecutive time domain pulses were acquired for each pressure level. The power spectra of each time domain signals weighted with rectangular window were calculated using fast Fourier transform (FFT). The average power spectra were computed for further analysis of the harmonics magnitudes. The harmonic tones are produced at an integer ( $n$ ) multiple of fundamental frequency,  $f$ . In our case, for a central frequency of 2.2 MHz, the harmonics are produced at: 4.4, 6.6, 8.8 MHz etc. Spectral noise was identified between the harmonic peaks, i.e. at  $((2n-1) \times f/2)$ , within the limits of  $\pm 0.2$  MHz. Liquid  $\leftrightarrow$  gas transition (ADV) was identified with the presence of stable cavitation of the gas filled MBs.

The primary goal of this study was to assess the threshold for ADV, i.e. the peak negative pressure value at which transition between liquid to gas core in the MBs occurs. Cavitation effects were evaluated using fundamental, second, third and fourth harmonic to noise ratio. Schematic representation of the method employed in this study is given in Fig. S6.

In Fig. S7 (a-d) the amplitude of the fundamental up to the fourth harmonic is reported. At low acoustic pressure, typically below 0.5 MPa, only fundamental response from the suspension has been detected. As peak negative pressure increases, second harmonic started to build up above a value of 0.61 MPa. Third and fourth harmonic were detected at a pressure value above 1 MPa, with a steep increase of the amplitude at pressures exceeding this value which has been assigned as the threshold for ADV and corresponds to an MI of 0.67, well below safety limit where medical ultrasound scanners usually work. It is worth mentioning that third and fourth harmonics are mostly attributed to the nonlinear oscillation of the gas bubbles. The lower value of the threshold pressure, 0.61 MPa, at which the second harmonic is observed, can be explained as a combined effect of nonlinear propagation of the acoustic wave through the walls of agarose vessel and gas bubbles. The ADV threshold presented in this work is in agreement with the results reported by Kripfgans et al.<sup>4</sup> for albumin stabilized droplets. Last, it should be noted that inertial cavitation or transient collapse of the bubble, that in frequency domain is characterized by the increase in broadband noise, was not observed at the pressure range considered in this study.

DexMA50 vesicle echogenicity was tested in an *in vitro* experiment using either 18 or 24 MHz transducers of the Vevo<sup>®</sup> 2100. In these experiments 5 mL of DexMA50 shelled vesicles were injected into a silicon tube with a constant flow rate maintained by a peristaltic pump calibrated at 2 mL/ min. Vevo<sup>®</sup> 2100 used parameters are summarized in Table S3.

Pre-processing consisted of two steps: i) the manual design of the lumen tube boundaries (*i.e.* the region of interest, ROIs). ROIs have been kept constant for all the images series; and ii) motion correction for video data and spatially realignment. Five ROIs were drawn in each image and their average intensity was computed. Data were normalized with respect to the first average value, corresponding to 4% of power. Custom developed software was used for the signal intensity analysis and applied for each ROI.

The acoustic behaviour of MBs was monitored by gradually increasing the power of US beam, related to the acoustic pressure. The signal intensity as a function of the power of the ultrasound

beam, from 4 % to 100% of system output, is shown in Fig. S8. The US image analysis highlighted a variation of MBs signal intensity correlated to the acoustic power value (strain or tension) of the ultrasound beam. This result is observed at 18 MHz frequency, while at 24 MHz the variations are negligible. This effect is related to the dimensions and composition of the MBs as described in eq 2:

$$f_r = \frac{1}{2\pi r} \cdot \sqrt{\frac{3\gamma P_{in}}{\rho}} \quad (2)$$

where  $\gamma$  and  $r$  are the ratio of specific heats of the gas core and the radius of MB, respectively,  $\rho$  is the density of the medium e  $P_{in}$  is the static pressure, relating the resonance frequency,  $f_r$ , to the Laplace pressure.<sup>5</sup>

### 10. Biodegradability of DexMA50 vesicles: lysozyme and dextranase effect

Biodegradation of DexMA50 vesicles was studied using two enzymes: lysozyme and dextranase. In a typical experiment with lysozyme, 6 mL of RBITC-labelled DexMA50 vesicles, prepared according to section 5, were centrifuged for 4 minutes at 1000 rpm. The supernatant was replaced with 1 mL of phosphate buffer solution (1 mM pH 7.4) containing  $1.44 \cdot 10^5$  IU/mL of lysozyme at 37 °C. The degradation was monitored by confocal microscopy. DexMA50 vesicles biodegradability was also tested using dextranase from *Penicillium sp.*, the  $\alpha(1-6)$ -D-glucosidase. The experiment was done on 6 mL of vesicles dispersion. After 4 minutes of centrifugation at 1000 rpm, supernatant was removed and replaced with 1 mL of dextranase solution 3.0 IU/mL in 0.1 N acetate buffer pH 5.5. Vesicles biodegradation by dextranase was monitored by using broad field microscope equipped with a chamber thermostated at 37°C using the “Perfect Focus System” (PFS) for accurate detection of a suitable axial reference plane for keeping focused the sample during the degradation process (see video, file name: DexMA50 1% dextranase20X002\_crop.avi.zip).

## 11. $^1\text{H}$ NMR spectrum of methacrylated-dextran

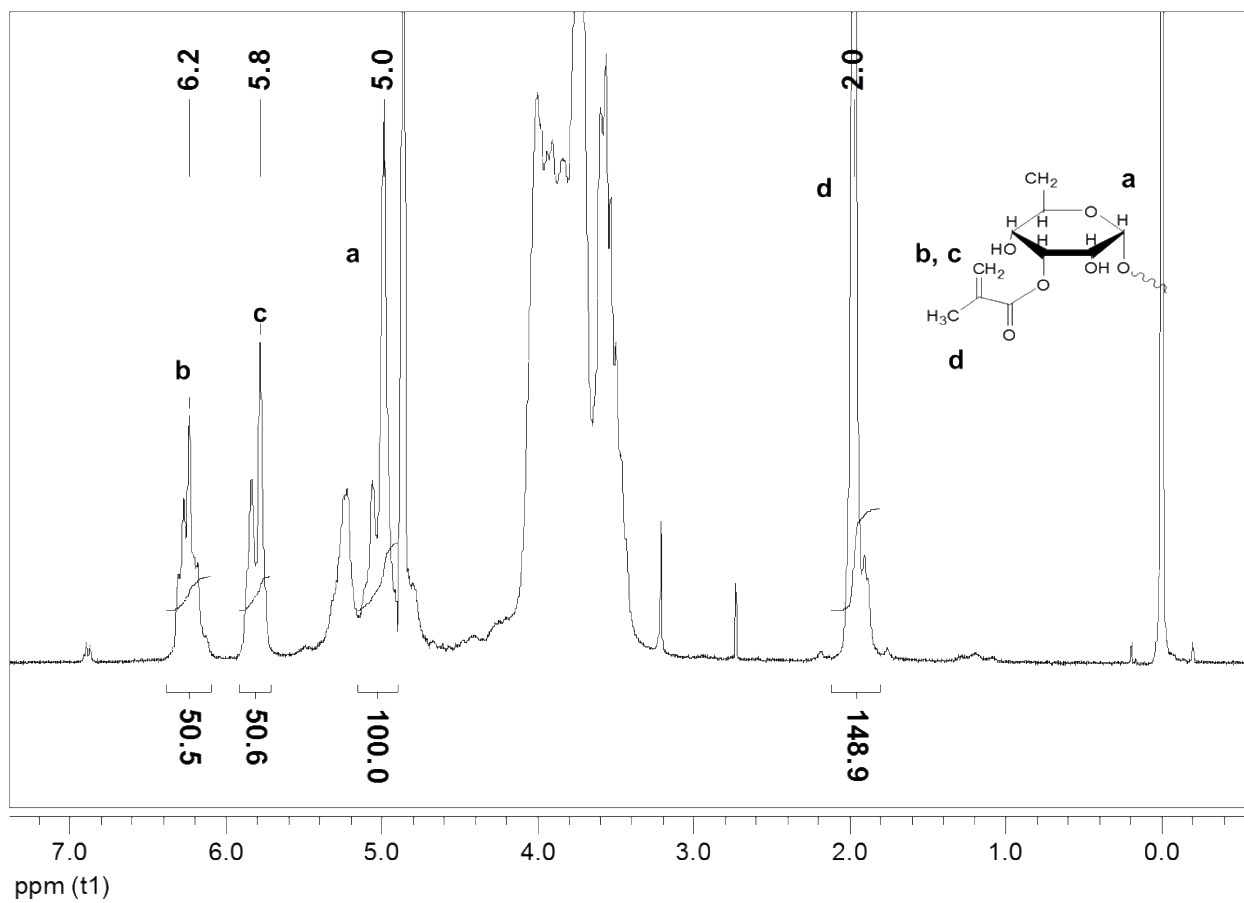


**Fig. S 1**  $^1\text{H}$  NMR spectrum of DexMA50 in  $\text{D}_2\text{O}$ . Resonances (b, c) were assigned to the vinyl protons of the acrylate moiety.

## 12. $^1\text{H}$ NMR spectrum of methacrylated-hyaluronic acid

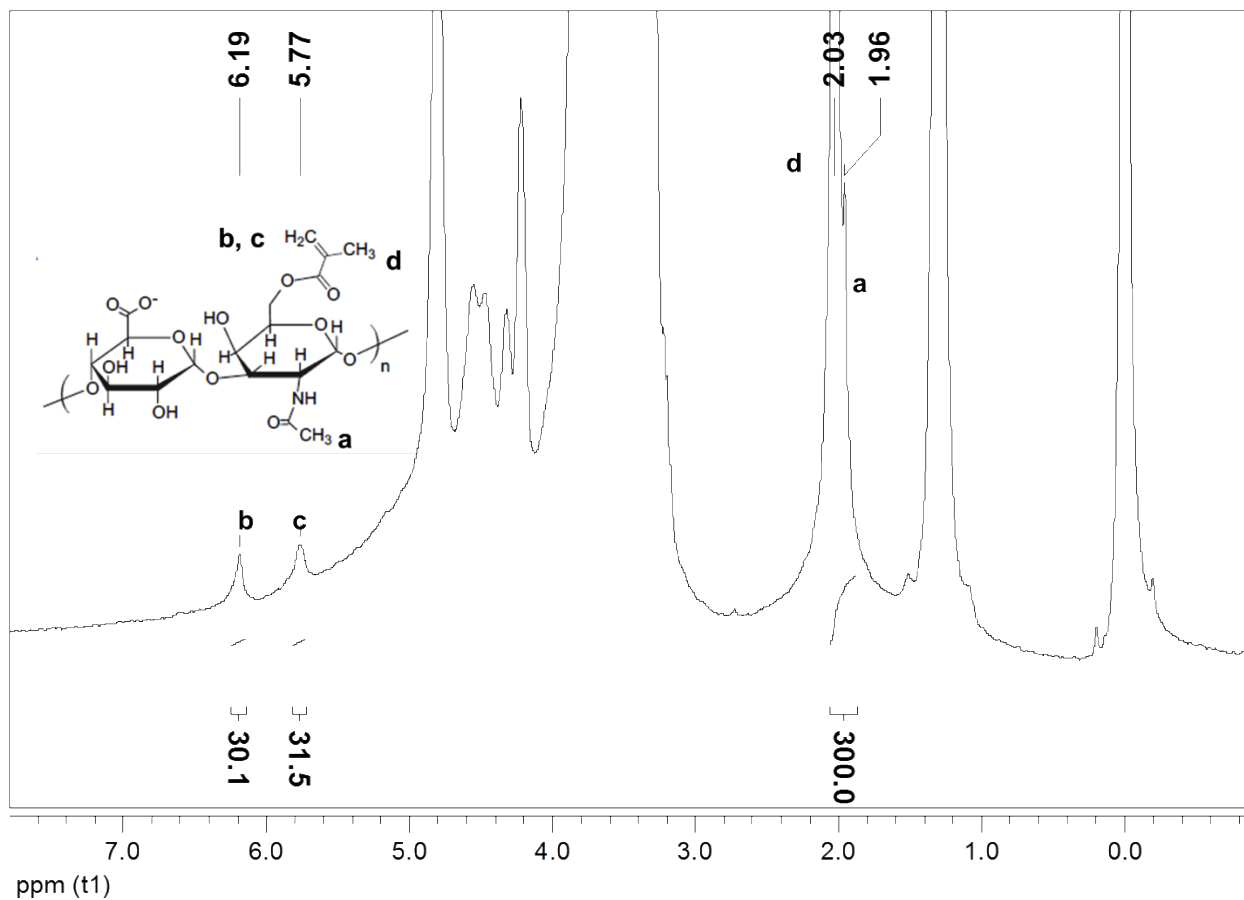


Fig. S 2  $^1\text{H}$  NMR spectrum of HAMA30 in  $\text{D}_2\text{O}$ .

### 13. Table S1: Composition (a) and parameters (b) set in vesicles synthesis

(a)

Vesicles	DexMA50	Dex/p(MA-co-NiPAAm)	HAMA30
Polymer (g/mL)	$10^{-2}$	$10^{-2}$ *	$5 \cdot 10^{-3}$
NiPAAm (g/mL)	-	$7 \cdot 10^{-3}$	-
Epikuron 200® (g/mL)	$5 \cdot 10^{-5}$	$5 \cdot 10^{-5}$	-
Palmitic Acid (g/mL)	$2 \cdot 10^{-5}$	$2 \cdot 10^{-5}$	-
Pluronic F127 (g/mL)	-	-	$5 \cdot 10^{-5}$
Octylamine (g/mL)	-	-	$2 \cdot 10^{-5}$
Decafluoropentane (g/mL)	$7 \cdot 10^{-2}$	$7 \cdot 10^{-2}$	$7 \cdot 10^{-2}$

\* NiPAAm/MA= 2.5 mol/mol

(b)

Vesicles	DexMA50	Dex/p(MA-co-NIPAM)	HAMA30
UltraTurrax speed (rpm)	13000	13000	15000
UltraTurrax time (min)	3	3	5
UV time (min)	20	20	20

#### 14. Table S2: SP100 parameters set in ultrasound treatment of vesicles

Experiment	Frequency (MHz)	Duty cycle	Intensity ( $\text{W} \cdot \text{cm}^{-2}$ )	Time (sec)
ADV	1	100 %	3.6	30
MBs Fracture	1	100 %	5.0	10

#### 15. Picture of ultrasound mediated fracture of DexMa50 vesicles

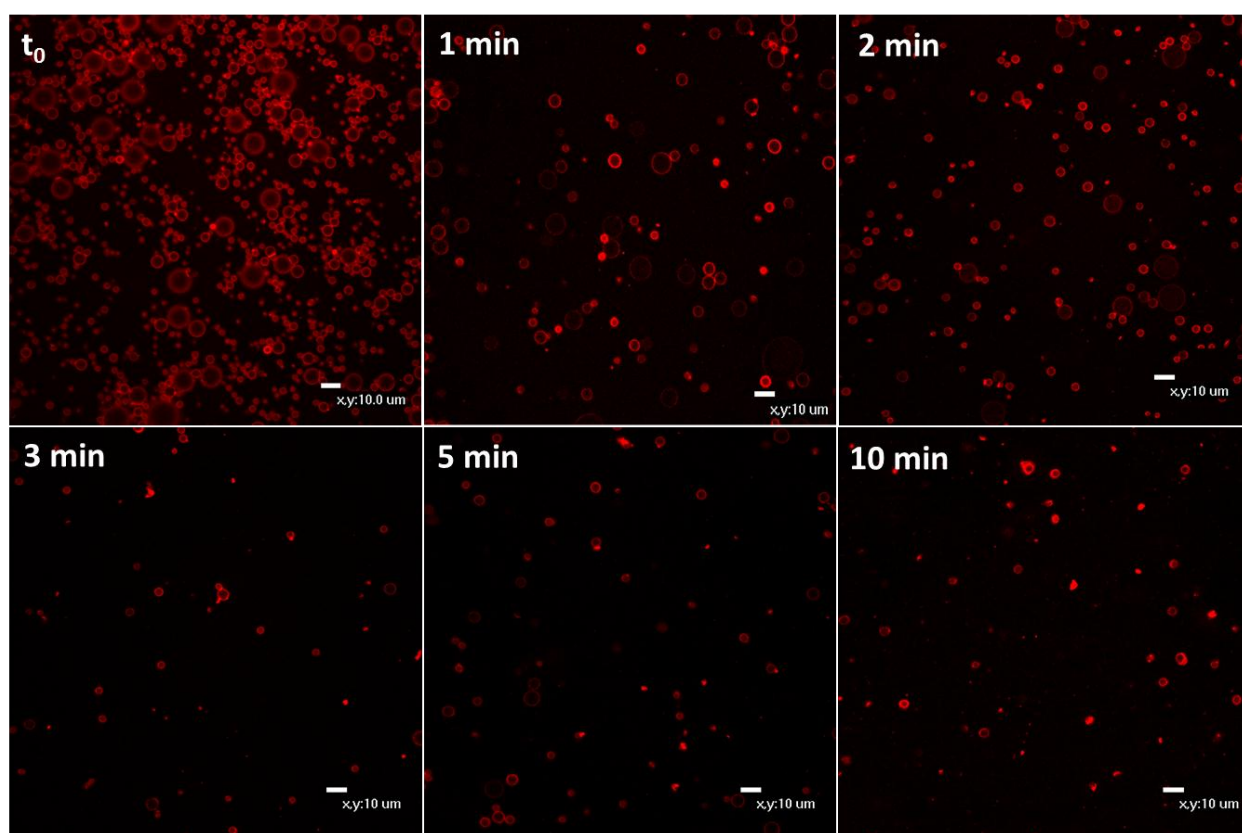
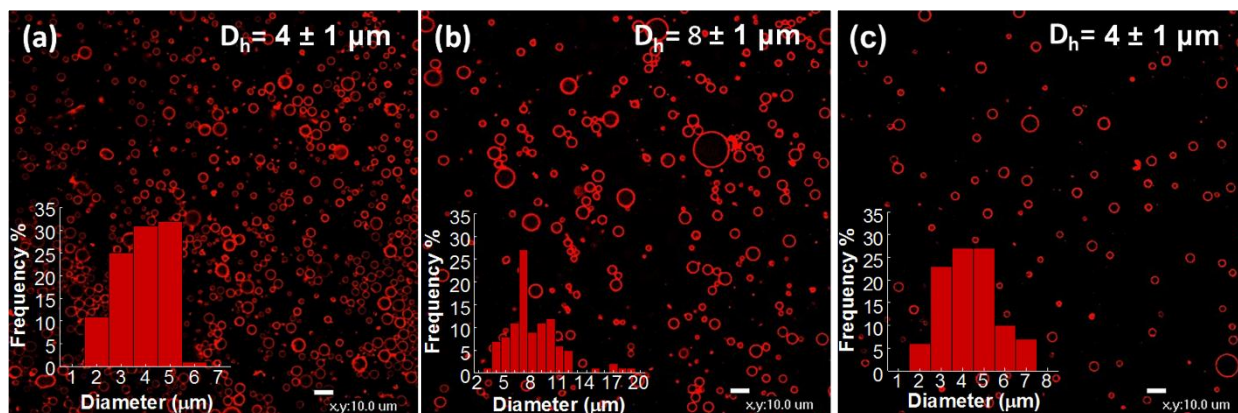


Fig. S 3 US induced fracture of RBITC-labelled DexMa50 vesicles.

## 16. Picture of ultrasound triggered ADV of Dex/p(MA-co-NiPAAm) vesicles



**Fig. S 4** Confocal microscopy of RBITC- labelled dex/p(MA-co-NiPAAm) shelled vesicles (a) before US irradiation, (b) after US irradiation and (c) one hour after US irradiation. Insets: size distributions and mean diameters.

## 17. Experimental set-up designed to simulate a harmonic imaging technique

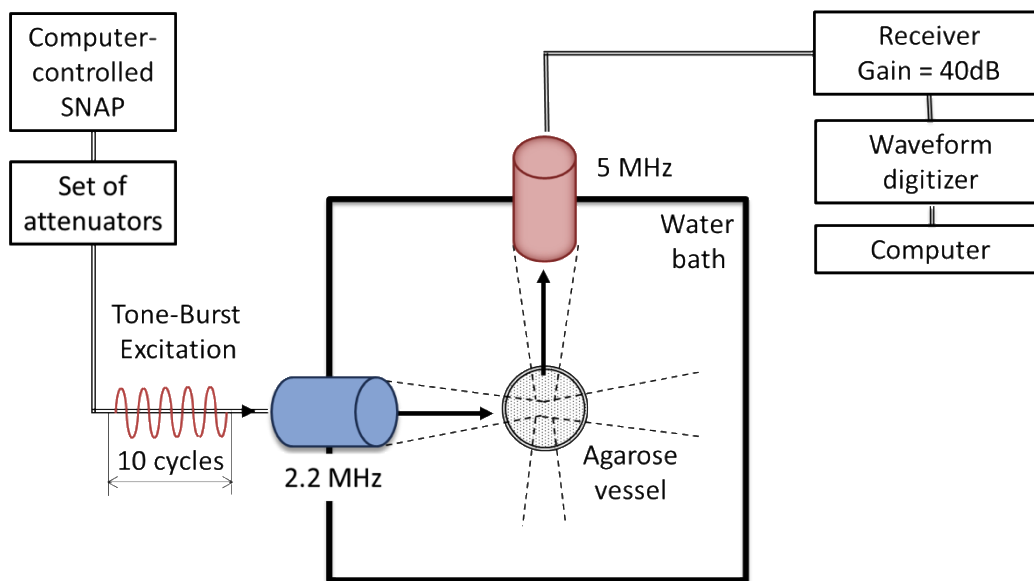


**Fig. S 5:** Scheme of the set up.

## 18. Pictures related to harmonic imaging technique simulation

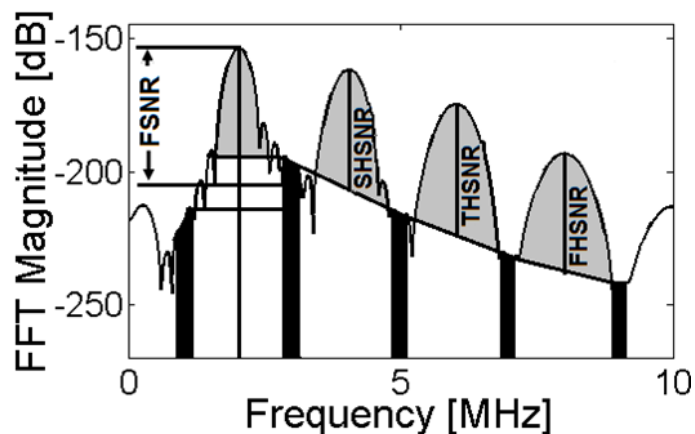


**Fig. S 6** Schematic representation of assessment of harmonic content of the spectra. Four ratios are reported in the scheme: fundamental to spectral noise ratio (FSNR), second harmonic to spectral noise ratio (SHSNR), third harmonic to spectral noise ratio (THSNR), and fourth harmonic to spectral noise ratio (FHSNR).

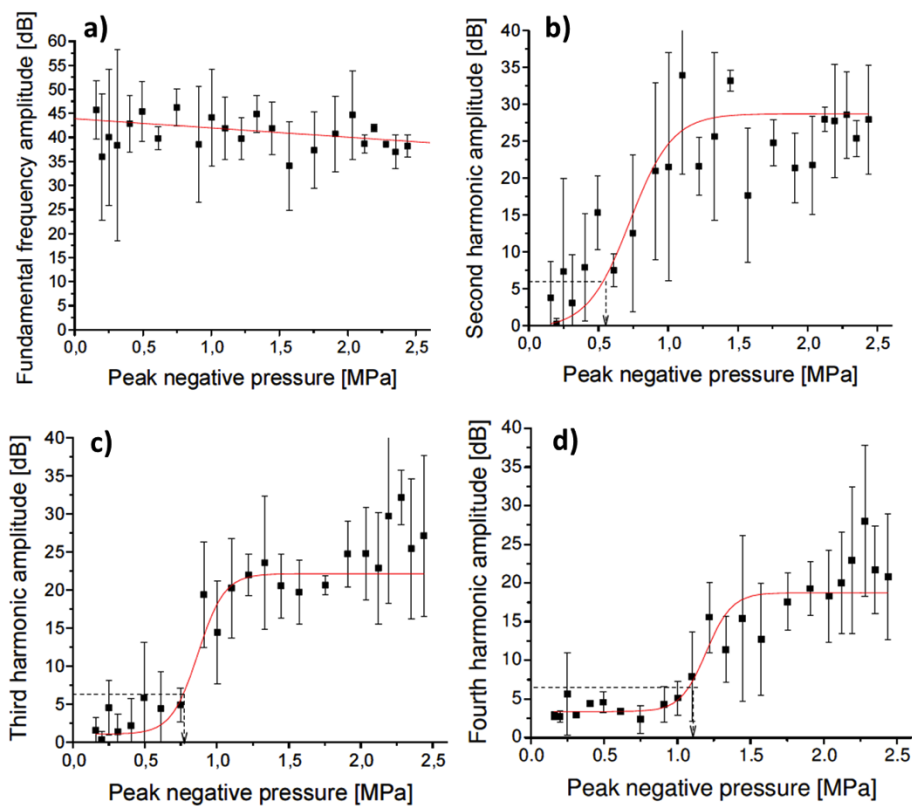


**Fig. S 7** Fundamental (a), second (b), third (c) and fourth (d) harmonics amplitudes as a function of applied negative pressure values. Bars represent standard deviations.

### 19. Table S3: Vevo<sup>®</sup> 2100 parameters set in micro-ultrasound experiment

Frequency (MHz)	Frame rate (fps)	Contrast gain (dB)
18	18	26
24	18	26

### 20. Picture of micro-ultrasound characterization performed by Vevo<sup>®</sup> 2100

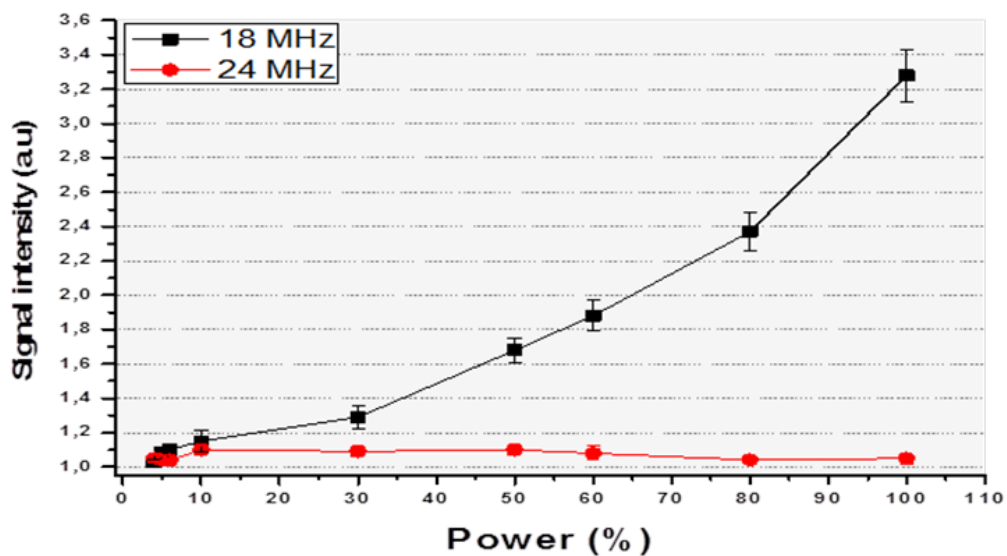


Fig. S 8 Normalized signal intensity as a function of the ultrasound power. Bars represent standard deviations.

## References

1. (a) W. N. E. van Dijk-Wolthius, J. J. Kettenes-van den Bosh, A. van der Ken-van Hoff and W. E. Hennink, *Macromolecules*, 1997, **30**, 3411; (b) W. N. E. van Dijk-Wolthius, O. Franssen, H. Talsma, M. Steenberger, J. J. Kettenes-van den Bosh and W. E. Hennink, *Macromolecules*, 1995, **26**, 6317.
2. S. A. Bencherif, A. Srinivasan, F. Horkay, J. O. Hollinger, K. Matyjaszewski and N. R. Washburn, *Biomaterials*, 2011, **29**, 1739.
3. D. O. Draper, J. C. Castel and D. Castel, *J. Orthop. Sports Phys. Ther.*, 1995, **22**, 142-150.
4. O. D. Kripfgans, J. B. Fowlkes, D. L. Miller, O. P. Eldevik and P. L. Carson, *Ultrasound Med. Biol.*, 2000, **26**, 1177.
5. A. A. Doinikov, J. F. Haac, and P. A. Dayton, *Ultrasonics*, 2009, **49**, 263.